

RESEARCH ARTICLE

The spectral features of EEG responses to transcranial magnetic stimulation of the primary motor cortex depend on the amplitude of the motor evoked potentials

Matteo Fecchio^{1☯‡}, Andrea Pigorini^{1☯‡}, Angela Comanducci¹, Simone Sarasso¹, Silvia Casarotto¹, Isabella Premoli^{2,3}, Chiara-Camilla Derchi¹, Alice Mazza¹, Simone Russo¹, Federico Resta⁴, Fabio Ferrarelli⁵, Maurizio Mariotti¹, Ulf Ziemann³, Marcello Massimini^{1,6}, Mario Rosanova^{1,7*}

1 Department of Biomedical and Clinical Sciences “L. Sacco”, University of Milan, Milan, Italy, **2** Department of Basic and Clinical Neuroscience, Institute of Psychiatry, Psychology and Neuroscience (IoPPN), King’s College London, London, United Kingdom, **3** Department of Neurology & Stroke, and Hertie Institute for Clinical Brain Research, University Tübingen, Tübingen, Germany, **4** Division of Radiology, Hospital Luigi Sacco, Milan, Italy, **5** Department of Psychiatry, University of Pittsburgh, Pittsburgh, United States of America, **6** IRCCS Fondazione Don Gnocchi Onlus, Milan, Italy, **7** Fondazione Europea per la Ricerca Biomedica Onlus, Milan, Italy

☯ These authors contributed equally to this work.
 ‡ These authors share first authorship on this work.
 * mario.rosanova@unimi.it



OPEN ACCESS

Citation: Fecchio M, Pigorini A, Comanducci A, Sarasso S, Casarotto S, Premoli I, et al. (2017) The spectral features of EEG responses to transcranial magnetic stimulation of the primary motor cortex depend on the amplitude of the motor evoked potentials. PLoS ONE 12(9): e0184910. <https://doi.org/10.1371/journal.pone.0184910>

Editor: Alessio Avenanti, University of Bologna, ITALY

Received: May 5, 2017

Accepted: September 1, 2017

Published: September 14, 2017

Copyright: © 2017 Fecchio et al. This is an open access article distributed under the terms of the [Creative Commons Attribution License](https://creativecommons.org/licenses/by/4.0/), which permits unrestricted use, distribution, and reproduction in any medium, provided the original author and source are credited.

Data Availability Statement: Preprocessed EEG dataset files containing anonymized TMS/EEG data for both experiments (experiment 1 and experiment 2) and each subject are available from Figshare database (DOI: [10.6084/m9.figshare.4970900.v1](https://doi.org/10.6084/m9.figshare.4970900.v1)).

Funding: This work has been partially funded by the LUMINOUS Project. This project has received funding from the European Union’s Horizon 2020 Research and Innovation Programme H2020-

Abstract

Transcranial magnetic stimulation (TMS) of the primary motor cortex (M1) can excite both cortico-cortical and cortico-spinal axons resulting in TMS-evoked potentials (TEPs) and motor-evoked potentials (MEPs), respectively. Despite this remarkable difference with other cortical areas, the influence of motor output and its amplitude on TEPs is largely unknown. Here we studied TEPs resulting from M1 stimulation and assessed whether their waveform and spectral features depend on the MEP amplitude. To this aim, we performed two separate experiments. In experiment 1, single-pulse TMS was applied at the same supra-threshold intensity on primary motor, prefrontal, premotor and parietal cortices and the corresponding TEPs were compared by means of local mean field power and time-frequency spectral analysis. In experiment 2 we stimulated M1 at resting motor threshold in order to elicit MEPs characterized by a wide range of amplitudes. TEPs computed from high-MEP and low-MEP trials were then compared using the same methods applied in experiment 1. In line with previous studies, TMS of M1 produced larger TEPs compared to other cortical stimulations. Notably, we found that only TEPs produced by M1 stimulation were accompanied by a late event-related desynchronization (ERD—peaking at ~300 ms after TMS), whose magnitude was strongly dependent on the amplitude of MEPs. Overall, these results suggest that M1 produces peculiar responses to TMS possibly reflecting specific anatomo-functional properties, such as the re-entry of proprioceptive feedback associated with target muscle activation.

FETOPEN-2014-2015-RIA under agreement No. 686764. This project has received funding from the European Union's Horizon 2020 Research and Innovation Programme under Grant Agreement No. 720270 (HBP SGA1). This study has been partially funded by the grant "Sinergia" CRSII3_160803/1 by the Swiss National Science Foundation, the James S. McDonnell Foundation Scholar Award 2013, and the Grant "Giovani Ricercatori" GR-2011-02352031 from the Italian Ministry of Health (to MR).

Competing interests: The authors have declared that no competing interests exist.

Introduction

The combination of Transcranial Magnetic Stimulation with electroencephalogram (TMS/EEG) allows recording the immediate response of the cerebral cortex to a focal perturbation with good spatial and temporal resolution [1]. Indeed, TMS-evoked EEG potentials (TEPs) provide a reliable read-out of the reactivity of cortical circuits provided that they are not confounded by scalp muscle artifacts or spurious sensory activations [2–4]. Typically, TEPs can last for hundreds of milliseconds and are characterized by sustained increases of power in frequency bands that specifically depend on the cortical target [5–8].

Over the last decade, several TMS/EEG studies have been conducted both on primary motor and sensory cortical areas [5,9–17] as well as associative cortical areas [6,7,18–22]. In this respect, the primary motor cortex (M1) has been largely used as the elective experimental model to study brain reactivity to TMS. However, the EEG response of M1 to TMS may represent a very special, instead of a representative case. In fact, the stimulation of M1 above resting motor threshold (RMT) [23,24] implies not only the excitation of cortico-cortical or cortico-thalamic circuits [5,9,13], but also the excitation of the corticospinal tract [25], which may, in turn, elicit motor evoked potentials (MEPs) and somatosensory feedback [26,27]. Moreover, M1 presents unique features in term of cytoarchitectonics, due to the strong presence of large V layer pyramidal cells [28,29] and the synaptic density/efficacy of corticospinal connections [30]. Previous studies have demonstrated that power and phase of ongoing EEG oscillations can modulate the amplitude of MEPs [31–33]. Other studies focused on possible relationship between specific TEPs components, in the time domain, possibly modulated by the presence of MEP. For instance, Paus et al. [15] found a positive correlation between MEP and absolute amplitude of N100, Maki et al. [14] found a significant correlation between N15-P30 and MEP amplitudes whereas Bonato et al. [34] did not find any correlation between early TEP components (N10, N18, and P30) and MEP amplitude. However, so far nobody investigated, in the time-frequency domain, if and how the amplitude of MEPs influences TEPs.

The present study aims at evaluating the specific characteristics of M1 TEPs compared to those of other cortical regions that do not elicit any peripheral output. Specifically, we performed two different experiments in order (i) to compare M1 TEPs to those elicited by prefrontal, premotor and parietal cortex stimulation and (ii) to test whether the TEPs generated by M1 stimulation are influenced by the related MEP amplitude. Compared to the other cortical areas, we found that TEPs recorded after stimulation of M1 were larger and characterized by a significant late broadband reduction of power in the time-frequency domain (event-related desynchronization—ERD). Importantly, we observed that larger MEPs were associated with larger TEPs and deeper ERD.

Materials and methods

Subjects

Six right-handed healthy subjects (3 female; age: 28 ± 3.6 years, values are given as mean \pm standard error here and in the following) took part in experiment 1 and a different group of six right-handed healthy subjects (2 female; age: 32 ± 3.0 years) participated in experiment 2 (see Experimental Procedure) after giving written informed consent. All volunteers were screened for contraindications to TMS during a physical and neurological examination [35]. Exclusion criteria included history of neurological or psychiatric disease, of CNS active drugs and abuse of any drug (including nicotine and alcohol). Experiments were approved by the Ethics Committee Milano Area A.

TMS targeting

In both experiments, a focal figure-of-eight coil (mean/outer winding diameter 50/70 mm, biphasic pulse shape, pulse length 280 μ s, focal area of the stimulation 0.68 cm²) connected to a Mobile Stimulator Unit (eXimia TMS Stimulator, Nexstim Ltd) was used to deliver single-pulse TMS. Stimulation sites included the middle frontal gyrus (Brodmann area [BA] 46), the superior frontal gyrus (BA 6), the precentral gyrus (BA 4) for M1, and the superior parietal gyrus (BA 7) on the left (motor dominant) hemisphere. All of these areas were anatomically identified on a T1-weighted individual magnetic resonance brain scan acquired with an Ingenia 1.5 T (Philips) scanner. For the left motor area, we stimulated the hand area corresponding to the abductor pollicis brevis muscle (APB) of the right hand, which was determined as the site where TMS consistently produced a selective muscle twitch. Stimulation parameters were controlled by means of a Navigated Brain Stimulation (NBS) system (Nexstim Ltd.) that employed a 3D, frameless infrared tracking-position sensor unit to display online, on the individual MRI scan, the position of the TMS coil with respect to the subject's head. NBS also estimated online the distribution and intensity (expressed in V/m) of the intracranial electric field induced by TMS and allowed to reliably control the stimulation coordinates, within and across sessions [36,37], by signaling in real-time any deviation from the designated target (error <3 mm). In order to standardize stimulation parameters, the maximum electric field was always kept on the convexity of the targeted gyrus with the direction of the induced current perpendicular to its main axis.

TEP and MEP recording

TEPs were recorded with a 60-channel TMS-compatible amplifier (Nexstim Ltd.), that prevents amplifier saturation and reduces, or abolishes, the magnetic artefacts induced by the coil's discharge [38]. The EEG signals were bandpass-filtered 0.1–350 Hz, sampled at 1450 Hz and referenced to an additional forehead electrode. Horizontal and vertical eye movements were recorded using two additional electrooculogram (EOG) sensors. Impedances at all electrodes were kept < 5 k Ω . As in previous studies, a masking noise capturing the specific time-varying frequency components of the TMS click was played via earphones throughout the entire TMS/EEG sessions to avoid contamination of the EEG signal by auditory potentials evoked [6,18,37]. The volume of the masking noise (always below 90dB) was increased until the subjects reported that the TMS click was not perceptible and was kept constant across stimulation sessions. The noise masking was interrupted during the inter-sessions intervals without removing the earplugs. Moreover, bone conduction was attenuated by placing a thin layer of foam between coil and scalp [39].

A 6-channel eXimia electromyography (EMG) system (3000 Hz sampling rate and 500 Hz cutoff for low-pass filtering) was used to record MEPs. Ag-AgCl self-adhesive electrodes were placed over the right APB muscle according to the belly-tendon montage [40].

Experimental procedures

During all TMS/EEG recordings, subjects were seated on a comfortable reclining chair, with eyes open and with the right hand positioned on a pillow placed over their lap. During stimulation of M1, subjects were instructed to keep the target muscle relaxed while EMG was continuously monitored on a computer screen.

In experiment 1, for every subject we performed 4 TMS/EEG measurements in which 4 cortical target were stimulated with a random order across subjects. For each TMS/EEG measurement we collected ~250 trials at an estimated electric field on the cortical surface of 120 V/m. To obtain this value, stimulation intensity, expressed as percentage of the maximal stimulator

output (MSO), was adjusted separately for each cortical target according to the scalp-to-cortex distance (prefrontal cortex = $65 \pm 4\%$ MSO and 16.2 ± 2.1 mm distance; premotor cortex: $69 \pm 3\%$ MSO and 15.7 ± 1.3 mm distance; motor cortex: $56 \pm 4\%$ MSO and 17.7 ± 1.5 mm distance; parietal cortex: $76 \pm 3\%$ MSO and 18.4 ± 2.0 mm distance). These values corresponded to 110% to 115% of resting motor threshold (RMT, defined as the minimum intensity necessary to elicit a peak-to-peak MEP amplitude higher than $50 \mu\text{V}$ in at least 5 out of 10 subsequent trials while muscle target is at rest, as assessed by the relative frequency method [23,24]). This intensity range is considered effective to produce significant EEG responses [36,37] and, at the same time, always evoked a clear but selective APB muscle twitch when targeting M1 (i.e. supra-threshold intensity). For each stimulation target, in experiment 1, inter-stimulus interval (ISI) randomly jittered between 3000 and 3300 ms. In experiment 2, M1 was stimulated with an ISI of 5000-5300ms (random jittering) to conform to the typical ISI used in the literature of M1 stimulation [41,42] and to reduce possible cumulative effects [43,44]. In experiment 2, a total number of 500 TMS pulses were delivered at RMT, corresponding to a mean estimated electric field of 93 ± 5.9 V/m across subjects. All stimulation sessions for both experiment 1 and experiment 2 were performed between late morning and early afternoon ($2:30\text{PM} \pm 1:45$) and subjects were not sleep-deprived nor drowsy at the time of the experiment.

Data analysis

For both experiments, data analysis was performed using Matlab R2012a (The MathWorks). Artifact-contaminated channels and trials were manually rejected by visual inspection [22] (in experiment 2, trial rejection also involved the visual inspection of single-trial MEPs). Then, EEG data were band-pass filtered (1–80 Hz, Butterworth, 3rd order), half-sampled at 725 Hz and segmented in a time window of ± 600 ms around TMS pulses. Bad channels were interpolated using EEGLAB spherical interpolation function [45] and signals were average re-referenced and baseline corrected (number of channels interpolated: 3 ± 2.5 in experiment 1, 3.7 ± 1.5 in experiment 2). Independent component analysis (ICA, EEGLAB *runica* function, [45]) was applied in order to remove residual eye blinks/movements and scalp muscle activations. In experiment 1, TEPs were obtained by averaging a minimum of 100 artifact-free single trials (170 ± 11 for prefrontal stimulation, 158 ± 16 for premotor stimulation, 118 ± 15 for M1 stimulation, 139 ± 18 for parietal stimulation, respectively).

In experiment 2, EMG traces were filtered (2 Hz high-pass, Butterworth, 3rd order) and segmented in a time window of ± 150 ms around the TMS pulse. Based on their peak-to-peak amplitude distribution across a large number of artifact-free trials (396 ± 19), for each session we averaged separately the 100 trials with the largest MEP amplitude (high-MEP condition) and the 100 trials with the smallest MEP amplitude (low-MEP condition).

In order to assess and compare the local TMS-evoked activity between stimulation sites and between high-MEP and low-MEP conditions, we first calculated the Local Mean Field Power (LMFP) computed as the square root of squared TEPs averaged across the four channels located under the stimulation coil (similar to [46]) and pertaining to the area of the scalp over each of the four cortical targets (F1-Fz-Fc1-Fcz for prefrontal cortex, Fc1-Fcz-C1-Cz for premotor cortex, C5-C3-Cp5-Cp3 for motor cortex and Cp1-Cpz-P1-Pz for parietal cortex). Then, we applied bootstrap statistics at the single subject level (number of permutations = 1000, $\alpha < 0.01$) on LMFP time-series obtained from all artifact free trials (see above), to estimate the LMFP values significantly different from the baseline (-500 to -100 ms (as in [47])). Specifically, the time samples of LMFP pre-stimulus (-500 to -100 ms) activity were shuffled at single trial level obtaining 1000 surrogated pre-stimulus LMFP time-series. Then, from each random

realization, the maximum value across all latencies was selected to obtain a maximum distribution (control for type I error) and significance level was set at $p < 0.01$. Significant activations were finally averaged between +8 and +350 ms and used for the group analysis of the local TEPs amplitude.

Spectral features were evaluated by computing the event-related spectral perturbation (ERSP) [45] between 8 and 45 Hz [6–8] after time-frequency decomposition using Wavelet transform (Morlet, 3.5 cycles). Absolute spectra normalization was applied first at the single-trial level performing a full-epoch length single-trial correction [48] and then by a pre-stimulus baseline correction (-500 to -100 ms) on the resulting ERSP averaged across all artifact free trials (see above), using the EEGLAB *newtimef* function [48]. This function also computes the surrogate distribution at each frequency by permuting baseline values, across both time and trials, and testing whether the original ERSP values point lie in the 0.5 or 99.5% tail of the surrogate distribution at any given frequency. If so, the specific time–frequency point is considered significant at $\alpha < 0.01$ after correction for multiple comparisons using the FDR procedure [48]. Finally, similar to LMFP, only significant ERSP values surviving this bootstrap-based statistics ($\alpha < 0.01$, number of permutations = 1000) with respect to baseline were considered in the group analysis. Specifically, for each of the stimulated cortical areas, we averaged the ERSP in the 8–45 Hz frequency range and in the time window between +200 and +350 ms, across the same four channels selected for LMFP calculation. This time range has been chosen based on the timing of the observed average (209 ± 17 ms) event related desynchronization (ERD) starting point (see [Results](#)).

Statistics

In experiment 1 significant differences among areas were assessed, for both LMFP and ERSP, by means of Kruskal–Wallis test and pairwise post-hoc Wilcoxon signed rank test were used (Bonferroni corrected). In experiment 2, statistical comparison between high-MEP and low-MEP conditions was performed on the LMFP and ERSP by means of paired Wilcoxon signed rank test.

Results

Experiment 1: M1 response to TMS is larger and characterized by distinct spectral features compared to the prefrontal, premotor, and parietal cortex responses

The local amplitude of TEPs, as measured by the significant LMFP values averaged between +8 and +350 ms, was significantly different among areas (Kruskal–Wallis test, $p = 0.0016$). Specifically, M1 stimulation elicited larger TEPs compared to the other stimulated sites (Wilcoxon signed rank test, $p < 0.05$, [Fig 1C](#)). The same results were obtained by contrasting the TEPs global amplitude across all 60 channels elicited by each stimulation site by means of the corresponding global mean field power (GMFP; Kruskal–Wallis test, $p = 0.0033$, see [S1 Fig](#)).

With respect to the EEG responses in the time-frequency domain (ERSP) we observed that all targeted cortical areas responded to TMS with a broadband increase of spectral power lasting up to ~200 ms ([Fig 1E](#)). After this first activation, spectral power returned to baseline in all targeted cortical areas except for M1, which showed a statistically significant event related desynchronization (ERD; blue color in top panel of [Fig 1D](#)). Across subjects, this ERD reached maximum values at about 300 ms post-TMS (310 ± 3.5 ms), as shown by the grand-average ERSP cumulated over the entire 8–45 Hz frequency range ([Fig 1E](#)). Indeed, statistical analysis showed that the modulation of spectral power was significantly different among areas

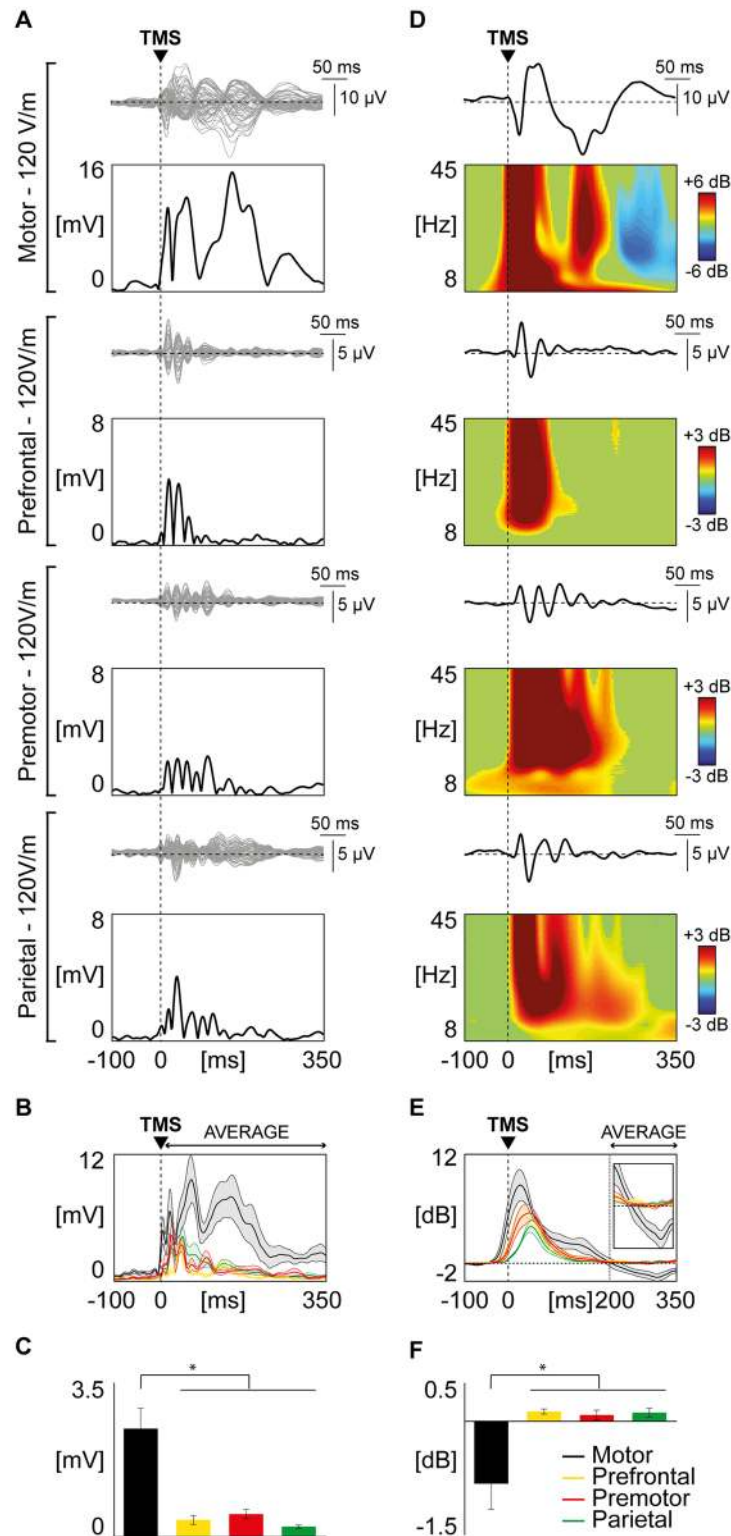


Fig 1. Comparison of TMS-evoked EEG potentials recorded from different cortical areas employing Local Mean Field Power (LMFP) and event-related spectral perturbation (ERSP). (A) For each stimulated area, TMS-evoked EEG responses are shown from one representative subject. Butterfly plots of all channels are displayed (top panels, grey traces), together with the corresponding LMFP (bottom panels, black traces). The dashed vertical line indicates the timing of the TMS pulse. **(B)** Grand-average of LMFP for each

stimulated area. Thick traces indicate the grand-average LMFP across subjects (\pm SE, color-coded shaded regions). Responses recorded after the stimulation of different cortical areas are color coded as follows: motor in black, prefrontal in yellow, premotor in red, parietal in green. **(C)** For each stimulated area, the LMFP values averaged between 8 and 350 ms post-TMS are shown in the bar histogram (mean \pm SE). Asterisks indicate statistically significant differences (* $p < 0.05$, Wilcoxon signed rank test). Bars are color coded as in Panel B. **(D)** Black traces represent TMS-evoked EEG responses of a representative subject (same as in panel A) for one of the four channels closest to the stimulation site, with the corresponding ERSP shown below. A Wavelet Transform (Morlet, 3.5 cycles) has been applied at the single trial level. Significance threshold for bootstrap statistics is set at $\alpha < 0.01$. Non-significant activity is set to zero (green), red colors indicate a significant increase with respect to the baseline, while blue colors indicate a significant reduction compared to the baseline. As in Panel A, the dashed vertical line indicates the time of the TMS pulse. **(E)** The averaged ERSP of the four channels located under the stimulation coil (between 8 and 45 Hz) is presented for each stimulated area (color coding as in panel B and C). Each thick line indicates the grand-average across subjects (\pm SE, color-coded shaded regions). The same traces are enlarged in the inset (time scale from 150 to 350 ms; power scale from -2 to 2 dB). The dashed vertical line indicates the average time in which the ERD occurs. **(F)** Using the same color coding as in panel B, C and E, bars indicate, for each stimulated area, the grand-average (\pm SE) of the averaged ERD (ERSP between 200 and 350 ms post-TMS). Asterisks indicate statistically significant differences (* $p < 0.05$, Wilcoxon signed rank test).

<https://doi.org/10.1371/journal.pone.0184910.g001>

(Kruskal–Wallis test, $p = 0.0027$) when averaged between +200 and +350 ms and that M1 modulation of power was significantly different from the average of the other stimulated sites (Wilcoxon signed rank test, $p < 0.05$; Fig 1F).

Both for LMFP and ERD, results at the group level are reproduced using the same number of trials (see S2 Fig).

Experiment 2: M1 responses to TMS are influenced by MEP amplitude

First, we replicated the M1-related ERD observations found in experiment 1 using a longer ISI (5000–5300 ms). Specifically, we observed that stimulating every 5000–5300 ms, M1 TEPs were characterized by a statistically significant late ERD averaged across the four channels closest to the stimulation site in the range of 8–45 Hz similar to that obtained using a shorter ISI (3000–3300 ms; S3 Fig).

Most importantly, for each session, the high number of recorded trials ($n = 500$) allowed to extract and analyze separately two subsets of 100 trials each, selected on the basis of the largest (high-MEP) and the smallest (low-MEP) single-trial MEP amplitude respectively. Across subjects, in the high-MEP condition the lowest MEP amplitude was on average 504 μ V (\pm 174 μ V), while in the low-MEP condition the highest amplitude was on average 165 μ V (\pm 38 μ V), therefore ensuring the absence of any overlap between high and low MEP conditions (Fig 2A, left panel). The average MEP amplitude for the high-MEP and low-MEP conditions were 1026 μ V (range 223–1527 μ V) and 29 μ V (range 4–72 μ V), respectively (Fig 2D, left panel).

The overall amplitude of TEPs, as measured by the average of significant LMFP values between +8 and +350 ms, was significantly reduced ($21.6 \pm 2.2\%$; Fig 2C) in low-MEP condition as compared to high-MEP condition (Wilcoxon signed rank test, $p < 0.05$) at the group level (Fig 2D, middle panel).

Regarding the effects of MEP amplitude on the spectral features of the local M1 EEG response, we found that the amount of ERD was significantly reduced (83.9 ± 22.9 ; Fig 2D, right panel) in the low-MEP condition as compared to the high-MEP condition (Wilcoxon signed rank test, $p < 0.05$). Notably, a topographic statistical analysis (Fig 3) indicated that the significant ERD reduction was confined (Wilcoxon signed rank test, $p < 0.05$) to the channels overlying the motor area (C3, C5, Cz, FC2, FC3 and FC5).

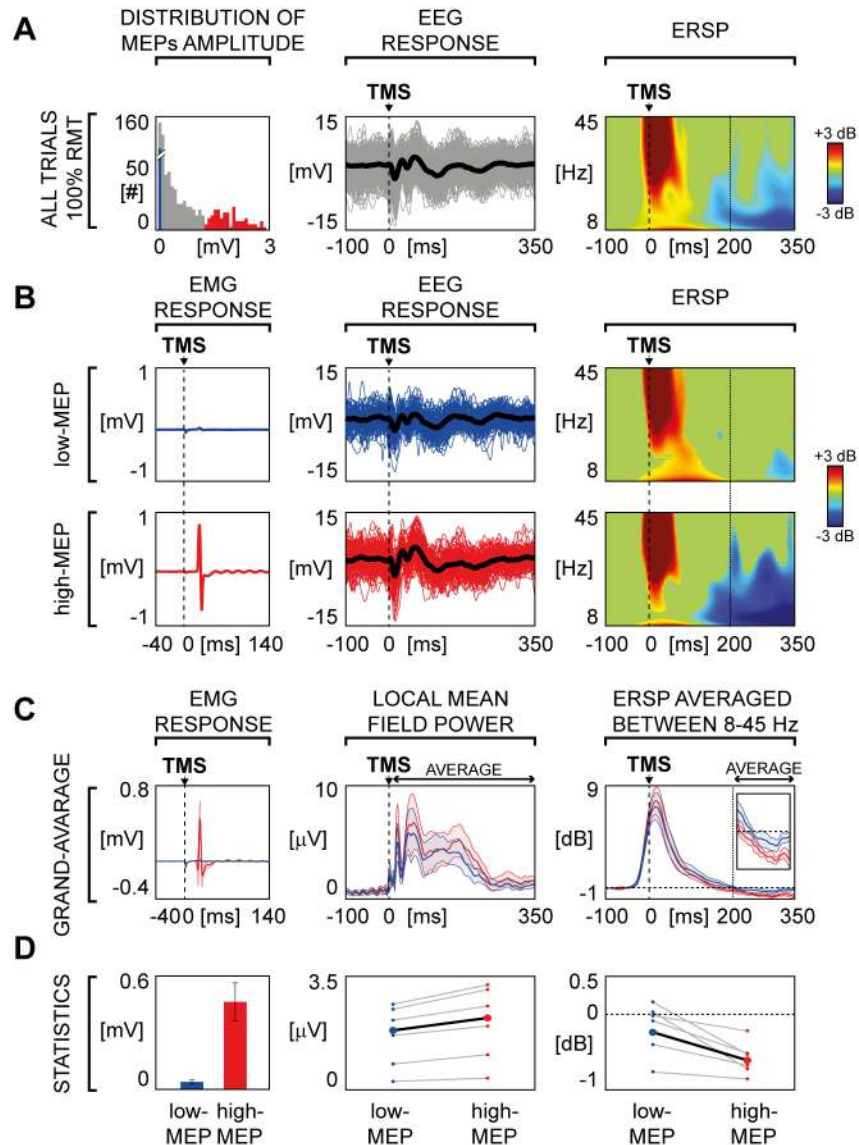


Fig 2. TMS-evoked EEG responses over left M1: Comparison between high-MEP and low-MEP conditions. (A) Left panel shows the distribution of the peak-to-peak MEPs amplitude of the all artifact-free trials for one representative subject. Blue bars correspond to 100 trials in which TMS elicited the smallest APB motor responses (low-MEP) and red bars corresponds to 100 trials in which TMS generated the largest APB motor responses (high-MEP). Then, from left to right, the EEG single trials (thin lines) and the average response (thick line) of the channel closest to the stimulation site (C3 scalp derivation) and the corresponding ERSP are shown. (B) For the same representative subject of Panel A, low-MEP (top panel) and high-MEP conditions (bottom panel) are compared. From left to right, the average MEP, the EEG single trials (thin lines) and average TEPs (thick line) recorded from the electrode closest to the stimulation site (C3 scalp derivation) and the corresponding ERSPs are shown. (C) MEP, LMFP and averaged ERSP derived from low-MEP (blue) and high-MEP (red) trials are compared. Each thick line indicates the grand-average across subjects (\pm SE, color-coded shaded regions). The averaged ERSP traces are enlarged in the inset (time scale from 150 to 350 ms; power scale from -1 to 1 dB). (D) From left to right: average (\pm SE) across subjects of the MEP peak-to-peak amplitude, individual averaged LMFP between 8 and 350 ms and the individual averaged ERSP between 200 and 350 ms are presented. Small circles and grey lines indicate single subject values, while large circles and black lines indicate grand-average values across subjects. Statistical analysis by means of Wilcoxon signed rank test resulted in significant differences for MEP ($p < 0.05$), LMFP ($p < 0.05$) and ERSP ($p < 0.05$).

<https://doi.org/10.1371/journal.pone.0184910.g002>

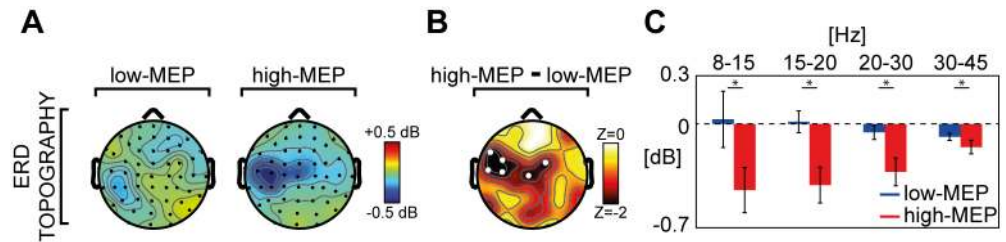


Fig 3. Comparison between low-MEP and high-MEP conditions across channels and frequency bands. (A) The broadband (8–45 Hz) ERD topography (ERSP averaged between 200 and 350 ms) of the grand-average across subjects derived from both low-MEP (left) and high-MEP conditions (right) is shown. (B) Topographic distribution of the z-values from a Wilcoxon signed rank test ($p < 0.05$) together with the statistical differences between the broadband ERD in the two conditions. The statistically significant electrodes (white dots) indicate that this broadband reduction was confined over the motor area (C3, C5, Cz, FC2, FC3 and FC5 scalp derivations). (C) For the significant channels of Panel B, the ERSP averaged between 200 and 350 ms across channels in the low-MEP (blue) and high-MEP (red) conditions over four EEG frequency bands (8–15 Hz, 15–20 Hz, 20–30 Hz, 30–45 Hz) are shown in the bar histogram (\pm SE). Asterisks indicate statistically significant differences (* $p < 0.05$, Wilcoxon signed rank test).

<https://doi.org/10.1371/journal.pone.0184910.g003>

Finally, splitting the average ERD over these six channels into four frequency bands (8–15 Hz, 15–20 Hz, 20–30 Hz, 30–45 Hz) we found significant differences between high-MEP and low-MEP conditions across all frequencies (Wilcoxon signed rank test, $p < 0.05$).

Discussion

In the present study, we investigated the peculiar features of the EEG responses of M1 to TMS and we asked whether those features are related to the amplitude of MEPs. To this aim we performed two series of experiments: in experiment 1 we compared TEPs of M1 with those of other cortical areas (premotor, prefrontal and parietal) in the time-frequency domain. Here stimulations were performed at an intensity of 120 V/m, which is largely above the threshold to reliably elicit a MEP. In experiment 2, we stimulated M1 at RMT and compared TEPs acquired within the same session and classified as low-MEP and high-MEP based on MEP amplitude. We found that: (i) according to previous studies [49] M1 TEP amplitude is larger as compared to any of the other stimulated areas, (ii) only the M1 response is associated with a late ERD (~300 ms), which is clearly modulated by the amplitude of MEPs. Although limited by the small sample size, these results are reproducible at the single subject level and are in line with previous similar studies.

Behavioral and electrophysiological measurements suggested that M1 is more excitable than other cortical areas [49–51]. For instance, previous works showed that TMS delivered above RMT over M1 and prefrontal cortex resulted in larger global response (GMFP) for the stimulation of M1 [49,51,52]. Here we confirmed and extended these results (experiment 1) by comparing TEPs of M1 to those generated by stimulating the premotor and posterior parietal cortices, which are usual targets in TMS/EEG experiments [6–8,53]. We observed that the M1 LMFP and GMFP to supra-threshold TMS (120 V/m as estimated by the neuronavigation system) are significantly larger than those measured after the stimulation of premotor and parietal cortices (Fig 1A–1C and S1 Fig).

Most important, the analysis of TEPs in the time-frequency domain showed that only the stimulation of M1 is associated to a statistically significant late (~300ms) broadband ERD (Fig 1D–1F), whose scalp topography is confined to the EEG electrodes overlying the stimulated sensory-motor areas (Fig 3). In terms of spectral and topographical features, the ERD we observed closely resemble the localized desynchronization of the ongoing EEG oscillations in

the low and high μ -bands induced by somatosensory stimulation [54] and by the execution of a voluntary movement [55]. Along the same lines, other studies showed that ERD in the β -band (15–30 Hz) recorded from sensory-motor cortices is associated with electrical nerve stimulation [56] and mechanical finger stimulation [57], as well as with movement and motor imagery [58,59]. At odds with these frequency-specific spectral profiles brought about by peripheral activations, the broadband ERD (Fig 3C) found in our study possibly reflects the direct cortical activation induced by TMS. Here, the ERD that hallmarks the electrical M1 response we recorded after supra-threshold TMS may be strongly contributed by the activation of specific cortico-spinal circuits [60] as well as by the sensory feedback from the activated muscle [54,57,61]. In order to further test this hypothesis, we performed a second set of measurements (experiment 2) in which TEPs following the stimulation of M1, at an intensity corresponding to RMT, were ranked based on the occurrence of high amplitude and low amplitude MEPs. Results clearly showed that in the high-MEP condition (i.e. when the cortico-spinal tract is more activated and the proprioceptive sensory feedback is stronger) the EEG response to TMS was significantly larger with respect to the low-MEP condition (i.e. when cortico-spinal tract is less activated and the proprioceptive sensory feedback is weaker), both in the early (as in [14]) and in the late TEP components (Fig 2C). Notably, also M1 ERD was influenced by the amplitude of MEPs, thus confirming a relationship between M1 EEG response to TMS and the effect of the stimulation at the peripheral level (Fig 2). Interestingly, when the stimulation of M1 did not trigger any muscular activation (as in [7]), the ERD was absent, confirming that the occurrence of ERD is only present when the stimulation actively involves the cortico-spinal tract (regardless the specific targeted muscle) and is associated with the proprioceptive sensory feedback, and absent otherwise (S4 Fig—see S1 Text).

More in general, the peculiar spectral properties of M1 response to TMS could be related to specific anatomic-functional features of the motor cortex, such as its high level of connectedness previously demonstrated by studies combining TMS with functional MRI [60,62]. In this case, the larger M1 EEG responses may be influenced by the activation of specific cortico-cortical pathways which involves areas directly connected to M1 such as the primary somatosensory cortex [63], the M1 contralateral to the stimulation, the supplementary motor and premotor areas [13,60,64]. With respect to the timing of the late ERD found in previous studies [56–58] and confirmed in the present work, its latency (~300ms) is consistent with the time interval required for the elaboration of the subjective awareness of somatosensory stimuli [65] further implying the role of sensory feedback on the specific M1 response to TMS. Altogether, these findings confirmed that the M1 EEG responses to TMS show peculiar features strongly related to the concurrent activation of a peripheral output.

In addition to these macro-anatomical aspects, also the peculiar M1 cytoarchitectonics may play a role. Indeed, magnetic stimulation seems to be more effective in exciting longitudinally oriented pyramidal cells which have a large-diameter myelinated axon and a wider dendritic tree [2,66]. Thus, the direct activation of giant Betz cells of layer Vb, whose strong presence is a unique feature of M1 [28,29], may contribute to the distinct features of M1 TEPs. Along these lines, future works should investigate whether both early and late M1-specific TEP-/ERSP-components may reflect peculiar M1 cytoarchitectonics and/or M1 circuitry properties unaffected by sensory feedback. Other studies could also explore the contributions of cytoarchitectonics and structural connectivity of other cortical areas, such as the occipital cortex [6], to the specificity of TEPs, towards the development of a non-invasive perturbational atlas.

Supporting information

S1 Text. Additional results.

(PDF)

S1 Fig. (A) Grand-average of GMFP for each stimulated area. Thick traces indicate the grand-average GMFP across subjects (\pm SE, color-coded shaded regions). Responses recorded after the stimulation of different cortical areas are color coded as follows: motor in black, prefrontal in yellow, premotor in red, parietal in green. (B) For each stimulated area, the GMFP values averaged between 8 and 350 ms post-TMS are shown in the bar histogram (mean \pm SE). Asterisks indicate statistically significant differences (* $p < 0.05$, Wilcoxon signed rank test). Bars are color coded as in Panel A.

(TIF)

S2 Fig. For each stimulated area, the LMFP values, calculated using all artifact free trials (panel A) and the same number of trials across stimulation site (panel B), and then averaged between 8 and 350 ms post-TMS are shown in the bar histogram (mean \pm SE). Asterisks indicate statistically significant differences (* $p < 0.05$, Wilcoxon signed rank test). Bars are color coded as in Fig 1. Using the same color coding for each stimulated area, the grand-average (\pm SE) of the averaged ERD, calculated using all artifact free trials (panel C) and the same number of trials across stimulation site (panel D). Asterisks indicate statistically significant differences (* $p < 0.05$, Wilcoxon signed rank test).

(TIF)

S3 Fig. Comparison of 5 second (top panels) and 3 second ISI (bottom panels) in one representative subject. For both ISIs, the distribution of peak-to-peak MEP amplitude of all artifact free trials (left top) and the corresponding average MEP (left bottom), the butterfly plots of all channels (right top, grey traces), the TEPs recorded at the channel closest to the stimulation site (right top, black traces) and the corresponding ERSPs (right bottom) are shown. Wavelet Transform (Morlet, 3.5 cycles) was applied at the single trial level. Significance threshold for bootstrap statistics is set at $\alpha < 0.01$. Non-significant activity was set to zero (green), red colors indicate a significant increase with respect to the baseline, while blue colors indicate a significant reduction with respect to the baseline. The dashed vertical line indicates the timing of the TMS pulse.

(TIF)

S4 Fig. Top and bottom panels show, for one representative subject, the average MEPs of the quadriceps and APB muscles, the butterfly plot of all channels (grey lines), the TEP of the channel closest to the stimulation site (black line) and the corresponding ERSP obtained by stimulating the medial M1 (leg motor cortex) respectively at 100% RMT_{APB} and 100% RMT_{Quadriceps}.

(TIF)

Acknowledgments

We thank Sasha D'Ambrosio, Thierry Nieuws and Renate Rutiku for insightful discussion and comments on the manuscript.

Author Contributions

Conceptualization: Matteo Fecchio, Andrea Pigorini, Angela Comanducci, Mario Rosanova.

Data curation: Matteo Fecchio, Isabella Premoli.

Formal analysis: Matteo Fecchio.

Funding acquisition: Marcello Massimini, Mario Rosanova.

Investigation: Matteo Fecchio, Andrea Pigorini, Angela Comanducci, Simone Sarasso, Chiara-Camilla Derchi, Alice Mazza, Simone Russo.

Methodology: Matteo Fecchio, Andrea Pigorini.

Project administration: Mario Rosanova.

Resources: Federico Resta.

Software: Matteo Fecchio, Andrea Pigorini.

Supervision: Maurizio Mariotti, Ulf Ziemann.

Validation: Silvia Casarotto, Fabio Ferrarelli.

Visualization: Matteo Fecchio, Andrea Pigorini.

Writing – original draft: Matteo Fecchio, Andrea Pigorini, Angela Comanducci, Mario Rosanova.

Writing – review & editing: Simone Sarasso, Silvia Casarotto, Fabio Ferrarelli, Ulf Ziemann, Marcello Massimini, Mario Rosanova.

References

1. Sejnowski TJ, Churchland PS, Movshon JA. Putting big data to good use in neuroscience. *Nat Neurosci.* 2014; 17: 1440–1441. <https://doi.org/10.1038/nn.3839> PMID: 25349909
2. Siebner HR, Hartwigsen G, Kassuba T, Rothwell JC. How does transcranial magnetic stimulation modify neuronal activity in the brain? Implications for studies of cognition. *Cortex.* 2009; 45: 1035–1042. <https://doi.org/10.1016/j.cortex.2009.02.007> PMID: 19371866
3. Ilmoniemi RJ, Kicić D. Methodology for combined TMS and EEG. *Brain Topogr.* 2010; 22: 233–248. <https://doi.org/10.1007/s10548-009-0123-4> PMID: 20012350
4. Gosseries O, Sarasso S, Casarotto S, Boly M, Schnakers C, Napolitani M, et al. On the cerebral origin of EEG responses to TMS: insights from severe cortical lesions. *Brain Stimul.* 2015; 8: 142–149. <https://doi.org/10.1016/j.brs.2014.10.008> PMID: 25481074
5. Van Der Werf YD, Paus T. The neural response to transcranial magnetic stimulation of the human motor cortex. I. Intracortical and cortico-cortical contributions. *Exp Brain Res.* 2006; 175: 231–245. <https://doi.org/10.1007/s00221-006-0551-2> PMID: 16783559
6. Rosanova M, Casali A, Bellina V, Resta F, Mariotti M, Massimini M. Natural frequencies of human corticothalamic circuits. *J Neurosci.* 2009; 29: 7679–7685. <https://doi.org/10.1523/JNEUROSCI.0445-09.2009> PMID: 19535579
7. Ferrarelli F, Sarasso S, Guller Y, Riedner BA, Peterson MJ, Bellesi M, et al. Reduced natural oscillatory frequency of frontal thalamocortical circuits in schizophrenia. *Arch Gen Psychiatry.* 2012; 69: 766–774. <https://doi.org/10.1001/archgenpsychiatry.2012.147> PMID: 22474071
8. Canali P, Sarasso S, Rosanova M, Casarotto S, Sferrazza-Papa G, Gosseries O, et al. Shared reduction of oscillatory natural frequencies in bipolar disorder, major depressive disorder and schizophrenia. *J Affect Disord.* 2015; 184: 111–115. <https://doi.org/10.1016/j.jad.2015.05.043> PMID: 26074020
9. Cracco RQ, Amassian VE, Maccabee PJ, Cracco JB. Comparison of human transcallosal responses evoked by magnetic coil and electrical stimulation. *Electroencephalogr Clin Neurophysiol.* 1989; 74: 417–424. [https://doi.org/10.1016/0168-5597\(89\)90030-0](https://doi.org/10.1016/0168-5597(89)90030-0) PMID: 2480220
10. Farzan F, Barr MS, Hoppenbrouwers SS, Fitzgerald PB, Chen R, Pascual-Leone A, et al. The EEG correlates of the TMS-induced EMG silent period in humans. *Neuroimage.* 2013; 83: 120–134. <https://doi.org/10.1016/j.neuroimage.2013.06.059> PMID: 23800790
11. Ferreri F, Rossini PM. TMS and TMS-EEG techniques in the study of the excitability, connectivity, and plasticity of the human motor cortex. *Rev Neurosci.* 2013; 24: 431–442. <https://doi.org/10.1515/revneuro-2013-0019> PMID: 23907420

12. Herring JD, Thut G, Jensen O, Bergmann TO. Attention Modulates TMS-Locked Alpha Oscillations in the Visual Cortex. *J Neurosci*. 2015; 35: 14435–14447. <https://doi.org/10.1523/JNEUROSCI.1833-15.2015> PMID: [26511236](https://pubmed.ncbi.nlm.nih.gov/26511236/)
13. Ilmoniemi RJ, Virtanen J, Ruohonen J, Karhu J, Aronen HJ, Näätänen R, et al. Neuronal responses to magnetic stimulation reveal cortical reactivity and connectivity. *Neuroreport*. 1997; 8: 3537–3540. <https://doi.org/10.1097/00001756-199711100-00024> PMID: [9427322](https://pubmed.ncbi.nlm.nih.gov/9427322/)
14. Mäki H, Ilmoniemi RJ. The relationship between peripheral and early cortical activation induced by transcranial magnetic stimulation. *Neurosci Lett*. 2010; 478: 24–28. <https://doi.org/10.1016/j.neulet.2010.04.059> PMID: [20435086](https://pubmed.ncbi.nlm.nih.gov/20435086/)
15. Paus T, Sipila PK, Strafella AP. Synchronization of neuronal activity in the human primary motor cortex by transcranial magnetic stimulation: an EEG study. *J Neurophysiol*. 2001; 86: 1983–1990. PMID: [11600655](https://pubmed.ncbi.nlm.nih.gov/11600655/)
16. Romei V, Murray MM, Merabet LB, Thut G. Occipital transcranial magnetic stimulation has opposing effects on visual and auditory stimulus detection: implications for multisensory interactions. *J Neurosci*. 2007; 27: 11465–11472. <https://doi.org/10.1523/JNEUROSCI.2827-07.2007> PMID: [17959789](https://pubmed.ncbi.nlm.nih.gov/17959789/)
17. Taylor PCJ, Walsh V, Eimer M. The neural signature of phosphene perception. *Hum Brain Mapp*. 2010; 31: 1408–1417. <https://doi.org/10.1002/hbm.20941> PMID: [20091790](https://pubmed.ncbi.nlm.nih.gov/20091790/)
18. Massimini M, Ferrarelli F, Huber R, Esser SK, Singh H, Tononi G. Breakdown of cortical effective connectivity during sleep. *Science*. 2005; 309: 2228–2232. <https://doi.org/10.1126/science.1117256> PMID: [16195466](https://pubmed.ncbi.nlm.nih.gov/16195466/)
19. Morishima Y, Akaishi R, Yamada Y, Okuda J, Toma K, Sakai K. Task-specific signal transmission from prefrontal cortex in visual selective attention. *Nat Neurosci*. 2009; 12: 85–91. <https://doi.org/10.1038/nrn.2237> PMID: [19098905](https://pubmed.ncbi.nlm.nih.gov/19098905/)
20. Mattavelli G, Rosanova M, Casali AG, Papagno C, Romero Lauro LJ. Top-down interference and cortical responsiveness in face processing: a TMS-EEG study. *Neuroimage*. 2013; 76: 24–32. <https://doi.org/10.1016/j.neuroimage.2013.03.020> PMID: [23523809](https://pubmed.ncbi.nlm.nih.gov/23523809/)
21. Harquel S, Bacle T, Beynel L, Marendaz C, Chauvin A, David O. Mapping dynamical properties of cortical microcircuits using robotized TMS and EEG: Towards functional cytoarchitectonics. *Neuroimage*. 2016; 135: 115–124. <https://doi.org/10.1016/j.neuroimage.2016.05.009> PMID: [27153976](https://pubmed.ncbi.nlm.nih.gov/27153976/)
22. Casarotto S, Comanducci A, Rosanova M, Sarasso S, Fecchio M, Napolitani M, et al. Stratification of unresponsive patients by an independently validated index of brain complexity. *Ann Neurol*. 2016; 80: 718–729. <https://doi.org/10.1002/ana.24779> PMID: [27717082](https://pubmed.ncbi.nlm.nih.gov/27717082/)
23. Groppa S, Oliviero A, Eisen A, Quartarone A, Cohen LG, Mall V, et al. A practical guide to diagnostic transcranial magnetic stimulation: report of an IFCN committee. *Clin Neurophysiol*. 2012; 123: 858–882. <https://doi.org/10.1016/j.clinph.2012.01.010> PMID: [22349304](https://pubmed.ncbi.nlm.nih.gov/22349304/)
24. Rossini PM, Burke D, Chen R, Cohen LG, Daskalakis Z, Di Iorio R, et al. Non-invasive electrical and magnetic stimulation of the brain, spinal cord, roots and peripheral nerves: Basic principles and procedures for routine clinical and research application. An updated report from an I.F.C.N. Committee. *Clin Neurophysiol*. 2015; 126: 1071–1107. <https://doi.org/10.1016/j.clinph.2015.02.001> PMID: [25797650](https://pubmed.ncbi.nlm.nih.gov/25797650/)
25. Di Lazzaro V, Ziemann U, Lemon RN. State of the art: Physiology of transcranial motor cortex stimulation. *Brain Stimul*. 2008; 1: 345–362. <https://doi.org/10.1016/j.brs.2008.07.004> PMID: [20633393](https://pubmed.ncbi.nlm.nih.gov/20633393/)
26. Rossi S, Pasqualetti P, Tecchio F, Sabato A, Rossini PM. Modulation of corticospinal output to human hand muscles following deprivation of sensory feedback. *Neuroimage*. 1998; 8: 163–175. <https://doi.org/10.1006/nimg.1998.0352> PMID: [9740759](https://pubmed.ncbi.nlm.nih.gov/9740759/)
27. Ellaway PH, Prochazka A, Chan M, Gauthier MJ. The sense of movement elicited by transcranial magnetic stimulation in humans is due to sensory feedback. *J Physiol*. 2004; 556: 651–660. <https://doi.org/10.1113/jphysiol.2003.060483> PMID: [14755003](https://pubmed.ncbi.nlm.nih.gov/14755003/)
28. Zilles K, Amunts K. Centenary of Brodmann's map—conception and fate. *Nat Rev Neurosci*. 2010; 11: 139–145. <https://doi.org/10.1038/nrn2776> PMID: [20046193](https://pubmed.ncbi.nlm.nih.gov/20046193/)
29. Chouinard PA, Paus T. The primary motor and premotor areas of the human cerebral cortex. *Neuroscientist*. 2006; 12: 143–152. <https://doi.org/10.1177/1073858405284255> PMID: [16514011](https://pubmed.ncbi.nlm.nih.gov/16514011/)
30. Maier MA, Armand J, Kirkwood PA, Yang H-W, Davis JN, Lemon RN. Differences in the corticospinal projection from primary motor cortex and supplementary motor area to macaque upper limb motoneurons: an anatomical and electrophysiological study. *Cereb Cortex*. 2002; 12: 281–296. <https://doi.org/10.1093/cercor/12.3.281> PMID: [11839602](https://pubmed.ncbi.nlm.nih.gov/11839602/)
31. Mäki H, Ilmoniemi RJ. EEG oscillations and magnetically evoked motor potentials reflect motor system excitability in overlapping neuronal populations. *Clin Neurophysiol*. 2010; 121: 492–501. <https://doi.org/10.1016/j.clinph.2009.11.078> PMID: [20093074](https://pubmed.ncbi.nlm.nih.gov/20093074/)

32. Giambattistelli F, Tomasevic L, Pellegrino G, Porcaro C, Melgari JM, Rossini PM, et al. The spontaneous fluctuation of the excitability of a single node modulates the internodes connectivity: a TMS-EEG study. *Hum Brain Mapp.* 2014; 35: 1740–1749. <https://doi.org/10.1002/hbm.22288> PMID: [23670997](https://pubmed.ncbi.nlm.nih.gov/23670997/)
33. Ferreri F, Vecchio F, Guerra A, Miraglia F, Ponzo D, Vollero L, et al. Age related differences in functional synchronization of EEG activity as evaluated by means of TMS-EEG coregistrations. *Neurosci Lett.* 2017; 647: 141–146. <https://doi.org/10.1016/j.neulet.2017.03.021> PMID: [28323091](https://pubmed.ncbi.nlm.nih.gov/28323091/)
34. Bonato C, Miniussi C, Rossini PM. Transcranial magnetic stimulation and cortical evoked potentials: a TMS/EEG co-registration study. *Clin Neurophysiol.* 2006; 117: 1699–1707. <https://doi.org/10.1016/j.clinph.2006.05.006> PMID: [16797232](https://pubmed.ncbi.nlm.nih.gov/16797232/)
35. Rossi S, Hallett M, Rossini PM, Pascual-Leone A. Screening questionnaire before TMS: an update. *Clin Neurophysiol.* 2011; 122: 1686. <https://doi.org/10.1016/j.clinph.2010.12.037> PMID: [21227747](https://pubmed.ncbi.nlm.nih.gov/21227747/)
36. Casali AG, Casarotto S, Rosanova M, Mariotti M, Massimini M. General indices to characterize the electrical response of the cerebral cortex to TMS. *Neuroimage.* 2010; 49: 1459–1468. <https://doi.org/10.1016/j.neuroimage.2009.09.026> PMID: [19770048](https://pubmed.ncbi.nlm.nih.gov/19770048/)
37. Casarotto S, Romero Lauro LJ, Bellina V, Casali AG, Rosanova M, Pigorini A, et al. EEG Responses to TMS Are Sensitive to Changes in the Perturbation Parameters and Repeatable over Time. *PLoS One.* 2010; 5: e10281. <https://doi.org/10.1371/journal.pone.0010281> PMID: [20421968](https://pubmed.ncbi.nlm.nih.gov/20421968/)
38. Virtanen J, Ruohonen J, Nääätänen R, Ilmoniemi RJ. Instrumentation for the measurement of electric brain responses to transcranial magnetic stimulation. *Med Biol Eng Comput.* 1999; 37: 322–326. <https://doi.org/10.1007/BF02513307> PMID: [10505382](https://pubmed.ncbi.nlm.nih.gov/10505382/)
39. ter Braack EM, de Vos CC, van Putten MJAM. Masking the Auditory Evoked Potential in TMS-EEG: A Comparison of Various Methods. *Brain Topogr.* 2015; 28: 520–528. <https://doi.org/10.1007/s10548-013-0312-z> PMID: [23996091](https://pubmed.ncbi.nlm.nih.gov/23996091/)
40. Preston D, Barbara S. *Electromyography and Neuromuscular Disorders.* Saunders; 2012.
41. Premoli I, Castellanos N, Rivolta D, Belardinelli P, Bajo R, Zipser C, et al. TMS-EEG Signatures of GABAergic Neurotransmission in the Human Cortex. *J Neurosci.* 2014; 34: 5603–5612. <https://doi.org/10.1523/JNEUROSCI.5089-13.2014> PMID: [24741050](https://pubmed.ncbi.nlm.nih.gov/24741050/)
42. Rothwell JC, Hallett M, Berardelli A, Eisen A, Rossini P, Paulus W. Magnetic stimulation: motor evoked potentials. *The International Federation of Clinical Neurophysiology. Electroencephalogr Clin Neurophysiol Suppl.* 1999; 52: 97–103. PMID: [10590980](https://pubmed.ncbi.nlm.nih.gov/10590980/)
43. Julkunen P, Säisänen L, Hukkanen T, Danner N, Könönen M. Does second-scale intertrial interval affect motor evoked potentials induced by single-pulse transcranial magnetic stimulation? *Brain Stimul.* 2012; 5: 526–532. <https://doi.org/10.1016/j.brs.2011.07.006> PMID: [21962979](https://pubmed.ncbi.nlm.nih.gov/21962979/)
44. Pellicciari MC, Miniussi C, Ferrari C, Koch G, Bortoletto M. Ongoing cumulative effects of single TMS pulses on corticospinal excitability: An intra- and inter-block investigation. *Clin Neurophysiol.* 2016; 127: 621–628. <https://doi.org/10.1016/j.clinph.2015.03.002> PMID: [25823698](https://pubmed.ncbi.nlm.nih.gov/25823698/)
45. Delorme A, Makeig S. EEGLAB: an open source toolbox for analysis of single-trial EEG dynamics including independent component analysis. *J Neurosci Methods.* 2004; 134: 9–21. <https://doi.org/10.1016/j.jneumeth.2003.10.009> PMID: [15102499](https://pubmed.ncbi.nlm.nih.gov/15102499/)
46. Casarotto S, Canali P, Rosanova M, Pigorini A, Fecchio M, Mariotti M, et al. Assessing the effects of electroconvulsive therapy on cortical excitability by means of transcranial magnetic stimulation and electroencephalography. *Brain Topogr.* 2013; 26: 326–337. <https://doi.org/10.1007/s10548-012-0256-8> PMID: [23053600](https://pubmed.ncbi.nlm.nih.gov/23053600/)
47. Rosanova M, Gosseries O, Casarotto S, Boly M, Casali AG, Bruno M-A, et al. Recovery of cortical effective connectivity and recovery of consciousness in vegetative patients. *Brain.* 2012; 135: 1308–1320. <https://doi.org/10.1093/brain/awr340> PMID: [22226806](https://pubmed.ncbi.nlm.nih.gov/22226806/)
48. Grandchamp R, Delorme A. Single-Trial Normalization for Event-Related Spectral Decomposition Reduces Sensitivity to Noisy Trials. *Front Psychol.* 2011; 2. <https://doi.org/10.3389/fpsyg.2011.00236> PMID: [21994498](https://pubmed.ncbi.nlm.nih.gov/21994498/)
49. Kähkönen S, Komssi S, Wilenius J, Ilmoniemi RJ. Prefrontal TMS produces smaller EEG responses than motor-cortex TMS: implications for rTMS treatment in depression. *Psychopharmacology (Berl).* 2005; 181: 16–20. <https://doi.org/10.1007/s00213-005-2197-3> PMID: [15719214](https://pubmed.ncbi.nlm.nih.gov/15719214/)
50. Boroojerdi B, Meister IG, Foltys H, Sparing R, Cohen LG, Töpper R. Visual and motor cortex excitability: a transcranial magnetic stimulation study. *Clin Neurophysiol.* 2002; 113: 1501–1504. [https://doi.org/10.1016/S1388-2457\(02\)00198-0](https://doi.org/10.1016/S1388-2457(02)00198-0) PMID: [12169333](https://pubmed.ncbi.nlm.nih.gov/12169333/)
51. Kähkönen S, Wilenius J, Komssi S, Ilmoniemi RJ. Distinct differences in cortical reactivity of motor and prefrontal cortices to magnetic stimulation. *Clin Neurophysiol.* 2004; 115: 583–588. <https://doi.org/10.1016/j.clinph.2003.10.032> PMID: [15036054](https://pubmed.ncbi.nlm.nih.gov/15036054/)

52. Komssi S, Kähkönen S, Ilmoniemi RJ. The effect of stimulus intensity on brain responses evoked by transcranial magnetic stimulation. *Hum Brain Mapp.* 2004; 21: 154–164. <https://doi.org/10.1002/hbm.10159> PMID: 14755835
53. Casula EP, Pellicciari MC, Ponzo V, Stampanoni Bassi M, Veniero D, Caltagirone C, et al. Cerebellar theta burst stimulation modulates the neural activity of interconnected parietal and motor areas. *Sci Rep.* 2016; 6: 36191. <https://doi.org/10.1038/srep36191> PMID: 27796359
54. Stancák A. Cortical oscillatory changes occurring during somatosensory and thermal stimulation. *Prog Brain Res.* 2006; 159: 237–252. [https://doi.org/10.1016/S0079-6123\(06\)59016-8](https://doi.org/10.1016/S0079-6123(06)59016-8) PMID: 17071235
55. Kuhlman WN. Functional topography of the human mu rhythm. *Electroencephalogr Clin Neurophysiol.* 1978; 44: 83–93. [https://doi.org/10.1016/0013-4694\(78\)90107-4](https://doi.org/10.1016/0013-4694(78)90107-4) PMID: 74329
56. Müller GR, Neuper C, Rupp R, Keinrath C, Gerner HJ, Pfurtscheller G. Event-related beta EEG changes during wrist movements induced by functional electrical stimulation of forearm muscles in man. *Neurosci Lett.* 2003; 340: 143–147. [https://doi.org/10.1016/S0304-3940\(03\)00019-3](https://doi.org/10.1016/S0304-3940(03)00019-3) PMID: 12668257
57. Gaetz W, Cheyne D. Localization of sensorimotor cortical rhythms induced by tactile stimulation using spatially filtered MEG. *Neuroimage.* 2006; 30: 899–908. <https://doi.org/10.1016/j.neuroimage.2005.10.009> PMID: 16326116
58. Pfurtscheller G, Berghold A. Patterns of cortical activation during planning of voluntary movement. *Electroencephalogr Clin Neurophysiol.* 1989; 72: 250–258. [https://doi.org/10.1016/0013-4694\(89\)90250-2](https://doi.org/10.1016/0013-4694(89)90250-2) PMID: 2465128
59. Pfurtscheller G, Neuper C, Ramoser H, Müller-Gerking J. Visually guided motor imagery activates sensorimotor areas in humans. *Neurosci Lett.* 1999; 269: 153–156. [https://doi.org/10.1016/S0304-3940\(99\)00452-8](https://doi.org/10.1016/S0304-3940(99)00452-8) PMID: 10454155
60. Shitara H, Shinozaki T, Takagishi K, Honda M, Hanakawa T. Movement and afferent representations in human motor areas: a simultaneous neuroimaging and transcranial magnetic/peripheral nerve-stimulation study. *Front Hum Neurosci.* 2013; 7. <https://doi.org/10.3389/fnhum.2013.00554> PMID: 24062660
61. Pfurtscheller G. Functional brain imaging based on ERD/ERS. *Vision Res.* 2001; 41: 1257–1260. [https://doi.org/10.1016/S0042-6989\(00\)00235-2](https://doi.org/10.1016/S0042-6989(00)00235-2) PMID: 11322970
62. Bohning DE, Shastri A, McConnell KA, Nahas Z, Lorberbaum JP, Roberts DR, et al. A combined TMS/fMRI study of intensity-dependent TMS over motor cortex. *Biol Psychiatry.* 1999; 45: 385–394. [https://doi.org/10.1016/S0006-3223\(98\)00368-0](https://doi.org/10.1016/S0006-3223(98)00368-0) PMID: 10071706
63. Petrichella S, Johnson N, He B. The influence of corticospinal activity on TMS-evoked activity and connectivity in healthy subjects: A TMS-EEG study. *PLoS ONE.* 2017; 12: e0174879. <https://doi.org/10.1371/journal.pone.0174879> PMID: 28384197
64. Komssi S, Aronen HJ, Huttunen J, Kesäniemi M, Soine L, Nikouline VV, et al. Ipsi- and contralateral EEG reactions to transcranial magnetic stimulation. *Clin Neurophysiol.* 2002; 113: 175–184. [https://doi.org/10.1016/S1388-2457\(01\)00721-0](https://doi.org/10.1016/S1388-2457(01)00721-0) PMID: 11856623
65. Libet B. Brain stimulation in the study of neuronal functions for conscious sensory experiences. *Human Neurobiology.* 1982; 1: 235–242. PMID: 6309708
66. Bonmassar G, Lee SW, Freeman DK, Polasek M, Fried SI, Gale JT. Microscopic magnetic stimulation of neural tissue. *Nat Commun.* 2012; 3: 921. <https://doi.org/10.1038/ncomms1914> PMID: 22735449